Calcium-Dependent Conformational Rearrangements and Protein Stability in Chicken Annexin A5

Javier Turnay,* Nieves Olmo,* María Gasset,† Ibón Iloro,‡ José Luis R. Arrondo,‡ and M. Antonia Lizarbe*
*Departamento de Bioquímica y Biología Molecular, Facultad de Ciencias Químicas, Universidad Complutense, 28040 Madrid, Spain; †Instituto Rocasolano de Química-Física, CSIC, 28006 Madrid, Spain; and ‡Unidad de Biofísica (Centro Mixto CSIC-UPV) y Departamento de Bioquímica, Universidad del País Vasco, Apdo. 644, 48080 Bilbao, Spain

ABSTRACT The conformational rearrangements that take place after calcium binding in chicken annexin A5 and a mutant lacking residues 3-10 were analyzed, in parallel with human annexin A5, by circular dichroism (CD), infrared spectroscopy (IR), and differential scanning calorimetry. Human and chicken annexins present a slightly different shape in the far-UV CD and IR spectra, but the main secondary-structure features are quite similar (70–80% α-helix). However, thermal stability of human annexin is significantly lower than its chicken counterpart (~8°C) and equivalent to the chicken N-terminally truncated form. The N-terminal extension contributes greatly to stabilize the overall annexin A5 structure. Infrared spectroscopy reveals the presence of two populations of α-helical structures, the canonical α-helices (~1650 cm^{-1}) and another, at a lower wavenumber (~1634 cm^{-1}), probably arising from helix-helix interactions or solvated α-helices. Saturation with calcium induces: alterations in the environment of the unique tryptophan residue of the recombinant proteins, as detected by near-UV CD spectroscopy; more compact tertiary structures that could account for the higher thermal stabilities (8 to 12°C), this effect being higher for human annexin; and an increase in canonical α-helix percentage by a rearrangement of nonperiodical structure or 3_{10} helices together with a variation in helix-helix interactions, as shown by amide I curve-fitting and 2D-IR.

INTRODUCTION

Annexins are a widely distributed multigene family of structurally related calcium binding proteins (for review, see Raynal and Pollard, 1994; Swairjo and Seaton, 1994; Gerke and Moss, 2002). Their main characteristic is the ability to reversibly bind to acid phospholipid-rich membranes in the presence of calcium. Several in vitro functions, including anticoagulatory and antiinflammatory activities, involvement in signal transduction, in membrane fusion, endo and exocytosis, and in calcium channel regulation have been described for these proteins, but little is known about their in vivo role (Raynal and Pollard, 1994; Gerke and Moss, 2002). However, some specific diseases, known as annexinopathies, have been described associated with abnormal expression of annexins A2 and A5; their study may contribute to a better understanding of the physiological role of these proteins (Rand, 1999). Some of these functions are specific for particular annexins, even though there is a high structural homology among them. Moreover, tissue-specific activities and alternatively spliced forms have been described for some particular annexins (Böhm et al., 1994; Sable and Riches, 1999). All members of this family of proteins present a highly conserved core structure composed of four (eight in annexin A6) homologous domains of ~70 amino acids showing a similar three-dimensional structure (Liemann and Huber, 1997). The main structural differences are located in their variable N-terminal region that differs greatly in length and amino acid sequence (Raynal and Pollard, 1994; Gerke and Moss, 2002). Annexin A5 crystal structure was the first one resolved (Huber et al., 1990); since then, several other annexins have been crystallized and all of them present an almost identical three-dimensional arrangement in the protein core. The molecules display a slightly bent disk shape where the four repeated domains, each of them comprising a four α-helix bundle (helices A, B, D, and E), are organized in a cylindrical way and are capped by a fifth α-helix (C).

The arrangement of the four domains allows the appearance of a central hydrophilic pore, which could be responsible for the voltage-dependent calcium channel activity reported for several annexins (A1, A2, A5–A7, B12) (Liemann et al., 1996; Hofmann et al., 1997; Matsuda et al., 1997). The interaction with membranes takes place on the convex side of the molecule where the main calcium-binding sites (one per domain) are located. The calcium ion binds to carbonyl oxygens in the loop connecting the A and B helices, and to a bidentate carboxyl group from a glutamic or aspartic acid residue located around 40 residues downstream in the loop connecting helices D and E. The N-terminal region is located in the opposite concave region of the annexin molecule binding together domains I and IV (Huber et al., 1990), at least in annexins with a short N-terminal domain, as annexin A5.

Taking into account that the main structural differences among annexins appear in the N-terminal extension, the search for specific functions of each annexin has been focused in this region. Annexin A5 presents the shortest N-terminal tail among all annexins described so far, only about 15 residues. In fact, it has been described that the

Submitted April 11, 2002, and accepted for publication May 29, 2002.

Address reprint requests to Prof. M. A. Lizarbe, Departamento de Bioquímica y Biología Molecular I, Facultad de Ciencias Químicas, Universidad Complutense, 28040 Madrid, Spain. Tel.: +34-91-3944148; Fax: +34-91-3944159; E-mail: lizarbe@bbm.1.ucm.es.

0006-3495/02/10/2280/12 $2.00

truncation of 14 residues of human annexin A5 (hA5) induces the loss of the calcium channel activity, suggesting the involvement of this region in the regulation of this channel (Berendes et al., 1993). On this idea, we have obtained and characterized a mutant chicken annexin A5 (dnt-cA5) lacking amino acid residues 3-10, being the secondary structure of this mutant almost identical to that of the wild-type protein (Turnay et al., 1995; Arboledas et al., 1997).

Calcium is essential for one of the main properties of annexins, their ability to bind to specific cellular membranes. Calcium requirements for half-maximal binding to phospholipid bilayers is highly variable among this family of proteins, ranging from submicromolar in annexin A2 to 10–100 μM in annexin A5 (Raynal and Pollard, 1994; Gerke and Moss, 2002). These calcium concentrations may be reached intracellularly under certain physiological conditions; however, calcium binding in the absence of phospholipids requires much higher concentrations of this cation (Raynal and Pollard, 1994; Sopkova et al., 1994). The crystal structure of domain III of annexin A5 reveals significant conformational changes upon calcium binding in the absence of phospholipids. Thus, the aim of this study is to analyze the effect of calcium binding, in the absence of phospholipids, in the stability and structure of annexin A5 and to get further insights into the role of the N-terminus in the maintenance of the overall structure of this protein. We have studied different structural and thermodynamic parameters of chicken annexin A5 (cA5) and dnt-cA5, comparing them with those of hA5.

MATERIALS AND METHODS

Protein preparation

Recombinant cA5 and its mutant dnt-cA5 have been produced and purified as previously reported (Turnay et al., 1995; Arboledas et al., 1997). hA5 cDNA was kindly provided by Dr. Pilar Fernández (University of Oviedo, Spain) and was subcloned as described for the chicken cDNA. Briefly, cDNAs were cloned into the pTrc99A prokaryotic expression vector (Amersham Pharmacia Biotech, Buckinghamshire, UK) and introduced into JA221 *Escherichia coli* strain cells. Expression was induced by addition of 1 mM isopropyl-β-D-thiogalactopyranoside (IPTG) for 16 h after the initial cultures reached 0.5 optical density at 550 nm. Recombinant proteins were purified from bacterial homogenates in the presence of 2.5 mM EGTA and using their ability to interact reversibly with phosphatidylserine-enriched liposomes (prepared from bovine brain extract, Folch fraction III, from Sigma, Alcobendas, Spain) in the presence of 2 mM calcium. A final DEAE-cellulose chromatography in 50 mM Tris, pH 7.4, containing 1 mM EGTA, was performed to further purify the protein preparations and to eliminate lipids. Pure annexin fractions were pooled and dialyzed against 20 mM Hepes, pH 7.4, containing 0.1 M NaCl and 1 mM EGTA, filtered through 0.22 μm membranes, and stored at 4°C until used. Before use, protein samples were dialyzed to equilibrium against buffer with or without calcium.

Circular dichroism measurements

Circular dichroism (CD) spectra were recorded in a Jasco J-715 spectropolarimeter at 25°C (Neslab RTE-111 thermostat). The far-UV CD spectra were monitored between 200 and 250 nm and near-UV CD spectra between 250 and 310 nm using 0.01 or 0.05 cm and 0.5 cm optical pathlength cuvettes for far- and near-UV, respectively. Melting curves were determined monitoring ellipticity changes at 222 nm between 25 and 75°C and increasing temperature at 60°C/h. Monitoring of ellipticity changes upon cooling from 75 to 25°C was also performed at 60°C/h. Spectra in the absence of calcium were recorded in 20 mM Hepes, pH 7.4, containing 0.1 M NaCl and 1 mM EGTA; titration of calcium influence in the near-UV was performed by sequential addition of a 0.5 M $CaCl_2$ stock solution (in 20 mM Hepes, pH 7.4, containing 0.1 M NaCl) and correcting the spectra for dilution. Checks were made to ensure that equilibrium was reached after each addition of calcium to the protein preparation. The influence of calcium concentration on the melting temperature was analyzed by preparing different protein samples from the same stock equilibrated at increasing calcium chloride concentrations. Samples with equivalent ionic strength obtained by addition of NaCl were used as controls. All spectra were obtained averaged over five scans (eight at low protein concentration) and were corrected by subtracting buffer contribution from parallel spectra in the absence of protein. The calcium-dependent variation in ellipticity at 292 nm, and in the melting curves recorded at 222 nm, was analyzed using a hyperbolic or logistic nonlinear regression fitting using SigmaPlot software (SPSS, Chicago, IL). Prediction of secondary structure from the far-UV CD spectra was performed using the convex constraint algorithm described by Perczel et al. (1992).

Infrared spectroscopy

Infrared spectroscopy (IR) spectroscopy measurements were performed on a Nicolet Magna II 550 spectrometer (Nicolet Instrument Corp., Madison, WI) equipped with a MCT detector, using a demountable liquid cell (Harrick Scientific, Ossining, NY) with CaF_2 windows and 50 μm spacers. A tungsten-copper thermocouple was placed directly onto the window and the cell placed in a thermostatted cell mount. Proteins were concentrated by ultrafiltration using Amicon Centriplus YM-10 membranes (10 kDa cutoff; Millipore, Bedford, MA) up to 20 mg/ml in 20 mM Hepes, pH 7.4, 0.1 M NaCl. Equilibration in D_2O buffer was achieved by protein lyophilization in the presence of buffer and reconstitution in D_2O with 99.8% isotopic enrichment (Merck, Darmstadt, Germany). Stock calcium solutions and buffer were also lyophilized and reconstituted in D_2O.

Thermal analyses were performed by heating continuously from 25 to 85°C at a rate of 60°C/h. Spectra were taken using a Rapid Scan software under OMNIC (Nicolet). For each degree of temperature interval, 305 interferograms were averaged, Fourier-transformed, and ratioed against a background, obtaining the spectra with a nominal resolution better than 2 cm^{-1}. Data treatment, band decomposition, and thermal analysis of the original amide I bands were performed as previously described (Arrondo et al., 1993; Arrondo and Goñi, 1999). After integrating each component, the corresponding percentages were obtained assuming that the molar absorption coefficients for the different protein structures were the same.

To obtain the 2D-IR maps, heating was used as the perturbation to induce time-dependent spectral fluctuations and to detect dynamical spectral variations on the secondary structure of annexin. Two-dimensional synchronous spectra have been obtained as described elsewhere (Contreras et al., 2001; Paquet et al., 2001).

Differential scanning calorimetry

Calorimetric measurements were performed in a Microcal MC-2 differential scanning calorimetry (DSC) microcalorimeter (Microcal, Northampton, MA) at a heating rate of 0.5°C/min between 25 and 85°C, and under

an extra constant pressure of 2 atm. Samples were always degassed for 15 min in a ThermoVac (Microcal) before loading into the calorimetric cell. The standard CpCalc, DA-2, and Microcal Origin packages were used for data acquisition and analysis. The excess heat capacity functions were obtained after baseline subtraction and correction for the instrument time response, as described previously (López Mayorga and Freire, 1987). The integration of the transition enthalpies (ΔH_{cal}) was done using Microcal Origin software, and the van't Hoff enthalpies (ΔH_{vH}) were calculated according to the van't Hoff equation for a monomolecular process:

$$\Delta H_{vH}(T_{1/2}) = 4RT_{1/2}^2 \frac{C_p(T_{1/2})}{\Delta H_{cal}(T_{1/2})} \quad (1)$$

where $T_{1/2}$ represents the temperature (K) at 50% of the peak area of the unfolding transition, $C_p(T_{1/2})$ and $\Delta H_{cal}(T_{1/2})$ are the molar excess heat capacity and transition enthalpy at $T_{1/2}$, respectively.

Protein samples were prepared at 0.3 mg/ml in 50 mM Hepes, pH 7.4, containing 0.1 M NaCl. EGTA or calcium concentrations were added by dialysis of the protein stock solution versus the corresponding buffer; after dialysis, protein concentration was determined. Due to the irreversibility of the thermal transitions, reheating scans were taken as baselines for each sample. Dialysis buffer was used to fill the reference cell and to perform the baseline run that preceded each sample run.

Other procedures

The purity of protein preparations was checked by silver-staining after polyacrylamide gel electrophoresis in the presence of sodium dodecylsulfate (SDS) according to Laemmli (1970). Protein concentration was determined by amino acid analysis (Beckman 6300 amino acid analyzer) or by recording UV-spectra and using extinction coefficients at 280 nm of 0.610, 0.615, and 0.590 ml·mg^{-1}·cm^{-1} for hA5, cA5, or dnt-cA5, respectively, after subtracting apparent absorption due to light scattering. Molar quantities have been calculated using molecular masses of 35,805, 36,067, and 35,160 Da for hA5, cA5, and dnt-cA5, respectively, according to the protein sequence.

RESULTS

Influence of calcium binding on the secondary structure of recombinant annexin A5

CD spectra in the far-UV region of cA5, dnt-cA5, and hA5 in the presence of 1 mM EGTA (absence of calcium), at 25°C and 75°C, and an additional spectrum for hA5 at 57°C in the absence of calcium are shown in Fig. 1. There are almost no differences between the CD spectra of the chicken wild-type protein and its N-terminally truncated mutant; analysis of the spectra using the CCA algorithm described by Perczel et al. (1992) reveals a very high α-helical percentage (~80%), a low contribution of β-turns, and the apparent absence of β-sheet structures in both recombinant proteins in the absence of calcium (Table 1). hA5 shows a slightly different spectrum with lower molar mean residue ellipticity and a higher ratio between the minima at 208 and 222 nm than chicken annexin, in which the ratio is close to one. Anyway, the analysis of the spectrum using the CCA algorithm also yields a similar content in α-helix.

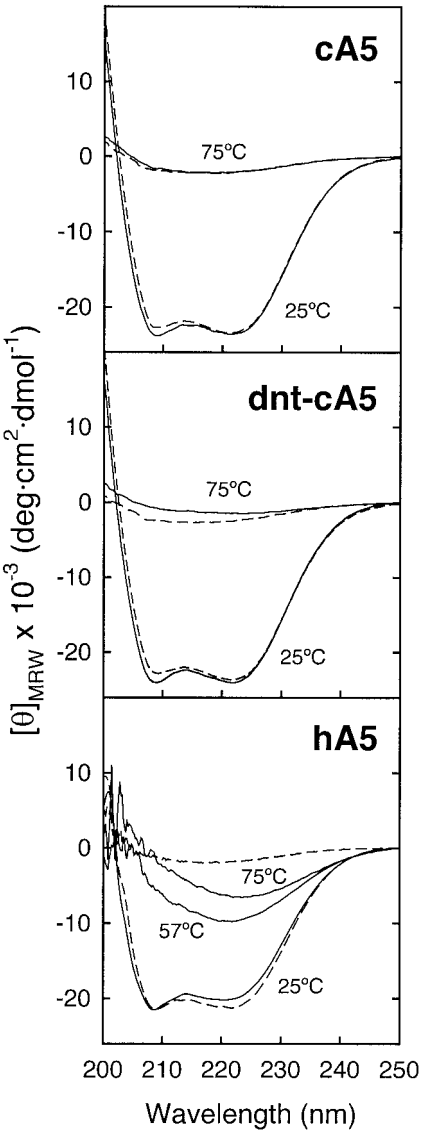

FIGURE 1 Far-UV circular dichroism spectra of recombinant annexins. CD spectra were recorded at 20 nm/min between 200 and 250 nm and are represented as mean residue weight ellipticities ($[\theta]_{MRW}$) in the absence (*solid lines*) or presence (*dashed lines*) of 100 mM $CaCl_2$ in 20 mM Hepes, pH 7.4, containing 0.1 M NaCl, at 25°C or 75°C (spectrum of hA5 at 57°C in the absence of calcium is also shown). Spectra are the average of five scans performed on a 0.05 cm optical pathlength cuvette using a protein concentration of ~0.7 mg/ml. No significant variations in the spectra were detected in the concentration range of 0.15–2.0 mg/ml. All spectra were corrected by subtracting ellipticities of the corresponding buffer solutions with or without calcium.

A preliminary study demonstrated that calcium concentrations up to 10 mM induced no significant changes in the spectra corresponding to wild-type cA5 and dnt-cA5 (Arboledas et al., 1997). However, even though this calcium concentration is really high compared to physiological values, it is not enough to reach saturation of calcium binding to annexin A5 in a phospholipid-free environment. We have

TABLE 1 Comparison of the secondary structures of chicken and human annexin A5 and dnt-cA5, based on far-UV CD spectroscopy, in the presence and absence of 100 mM $CaCl_2$

Protein	Structure			
Far-UV CD Spectroscopy	α-Helix (%)	β-Sheet (%)	β-Turns (%)	Random (%)
cA5	80	1	5	14
cA5 + 100 mM $CaCl_2$	87	3	7	3
dnt-cA5	81	0	5	14
dnt-cA5 + 100 mM $CaCl_2$	86	5	5	4
hA5	78	0	11	11
hA5 (57°C)	18	51	0	31
hA5 + 100 mM $CaCl_2$	83	4	6	7

The secondary structure composition was derived from the analysis of the far-UV CD spectra using the CCA algorithm or as described under Materials and Methods. At least three different protein preparations of each recombinant protein were analyzed and the relative error in the percentages of secondary structure was in all cases ~5%.

recorded the spectra of the three recombinant proteins at increasing calcium concentrations up to 100 mM. Fig. 1 shows only the spectra in the absence or presence of 100 mM calcium. Small gradual but significant changes in the band shape of the amide UV CD spectra are observed with the addition of calcium to the chicken proteins. However, the hA5 band shape changed at relatively low calcium (5 mM), remaining unchanged thereafter, as also reported previously (Sopkova et al., 1994). These changes have been detected not only working with different protein preparations, but also with concentrations ranging from 0.15 to 2 mg/ml. While molar ellipticities at 222 nm are almost constant for chicken annexins ($-23{,}566 \pm 198$ and $-24{,}051 \pm 206$ deg·cm^2·dmol^{-1} for the wild-type and dnt-cA5, respectively), a decrease in molar ellipticity at 208 nm is observed by ~6% of the original values. For hA5, CD spectra increase the negative CD intensity at 222 nm by 6.5% of the original value, remaining ellipticity at 208 nm almost constant. Analysis of the spectra in the presence of 100 mM calcium (Table 1) shows in all cases a slight increase in the α-helical percentage (7% for cA5, 5% for dnt-cA5 and hA5) with a parallel decrease in random structure and also a slight variation in β-turns, as deduced from the predictions according to the CCA algorithm.

Thermal unfolding of annexin A5 followed by far-UV CD spectroscopy

The thermal unfolding of the recombinant proteins was followed by monitoring the changes in molar ellipticity at 222 nm (Fig. 2). Thermal unfolding was highly cooperative and, in all cases, irreversible, as deduced from the data obtained during the cooling process from 75°C to 25°C (data not shown). The melting temperature (T_m) of the chicken wild-type protein in the absence of Ca^{2+} is 59.2 ± 0.4°C, whereas it is only 52.0 ± 0.3°C for dnt-cA5 (Fig. 2). Under identical experimental conditions, we have deter-

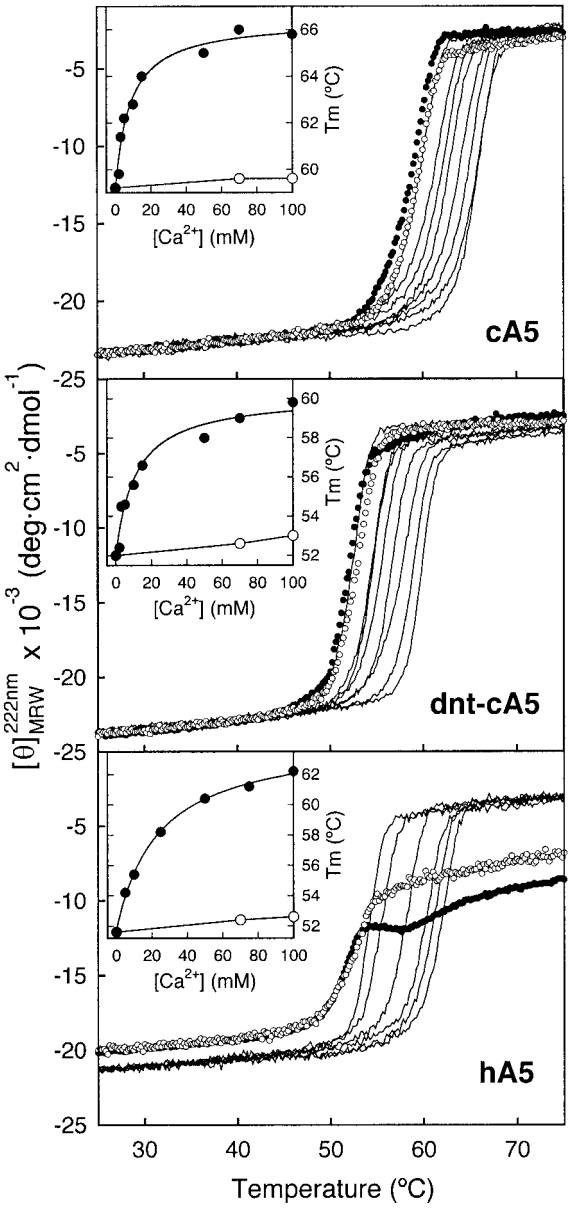

FIGURE 2 Influence of calcium binding on the thermal melting curves of recombinant annexins. Denaturing curves were obtained by monitoring the molar ellipticities per residue at 222 nm on a 0.05 cm optical pathlength thermostatted cuvette and a heating rate of 60°C/min. Independent protein samples (0.7 mg/ml) were prepared from the same stock at different calcium concentrations in 20 mM Hepes, pH 7.4, 0.1 M NaCl. The different calcium concentrations used for each melting curve (range 0–100 mM) correspond to those indicated in the insets. Melting curves corresponding to the recombinant proteins in the absence of calcium are drawn as filled circles. The curves corresponding to proteins in buffer containing 0.4 M NaCl (ionic strength equivalent to 100 mM $CaCl_2$ in buffer) are shown in open circles. *Insets*: Dependence of the melting temperature with $CaCl_2$ concentration (*filled circles*) and with an ionic strength equivalent to buffer containing 70 and 100 mM $CaCl_2$ obtained by increasing NaCl concentration (*open circles*).

mined that hA5 presents a melting temperature of only 51.6 ± 0.3°C, which is consistent with previously reported data obtained by DSC and IR studies (Vogl et al., 1997; Rosengarth et al., 1999; Wu et al., 1999). However, in hA5, an apparent biphasic behavior in the melting curve is detected in contrast to chicken proteins (Fig. 2). From 55°C to 57.5°C, a stabilization of the molar ellipticity at 222 nm can be observed, increasing again thereafter with a new inflection point at 60.8°C. Analysis of the far-UV CD spectrum of this putative intermediate state of hA5 (Fig. 1) yields a 18% of α-helix, 51% of β-sheet structure, and 31% of unordered structure (Table 1). The transition from the native structure to this intermediate state is also irreversible, as deduced from denaturing experiments in which temperature was increased to 57°C and then lowered. Molar ellipticity remained unchanged during the cooling ramp, and no refolding was detected.

The effect of calcium binding on the thermal stability of the chicken and human recombinant proteins was also analyzed. Even though only small variations in the secondary structure were detected, proteins were much more stable in the saturated Ca^{2+}-bound form. This effect is specific for calcium binding and is not due to changes in the ionic strength; controls with equivalent ionic strength, obtained by increasing NaCl concentration, show only a minor variation in the melting temperatures (Fig. 2). In hA5, the increase in ionic strength with NaCl does not alter the melting temperature, but changes the shape of the melting curve with a disappearance of the apparently biphasic behavior (Fig. 2). A titration of the effect of calcium up to 100 mM is also shown in Fig. 2. Saturation of this effect, as deduced from the nonlinear regression fitting of the experimental data to 3-parameter hyperbola, is achieved at 67.2 ± 2.4°C and 60.2 ± 4.3°C for cA5 and dnt-cA5, respectively, and 64.2 ± 0.9°C for hA5. The half-maximal effect of calcium in the denaturing curve of these proteins is lower for the chicken wild-type protein (8.2 ± 2.0 mM) followed by its mutant (11.9 ± 2.8 mM), and was higher for hA5 (23.6 ± 0.5 mM).

Influence of calcium binding on the W^{187} environment

To check possible differences in W^{187} exposure with calcium among the different annexins herein studied, we have recorded near-UV CD spectra as a function of calcium concentration. Spectra in the absence and presence of increasing concentrations of $CaCl_2$ are shown in Fig. 3, *A–C*. The spectra of the recombinant proteins in the presence of 1 mM EGTA or 0.4 M NaCl (ionic strength equivalent to buffer containing 100 mM $CaCl_2$ and 0.1 M NaCl) are identical to the spectra obtained in the absence of calcium and, thus, they have not been included. All these spectra present a maximum at 292 nm and four minima at 262, 269, 277, and 285 nm. Significant changes in the spectra can be

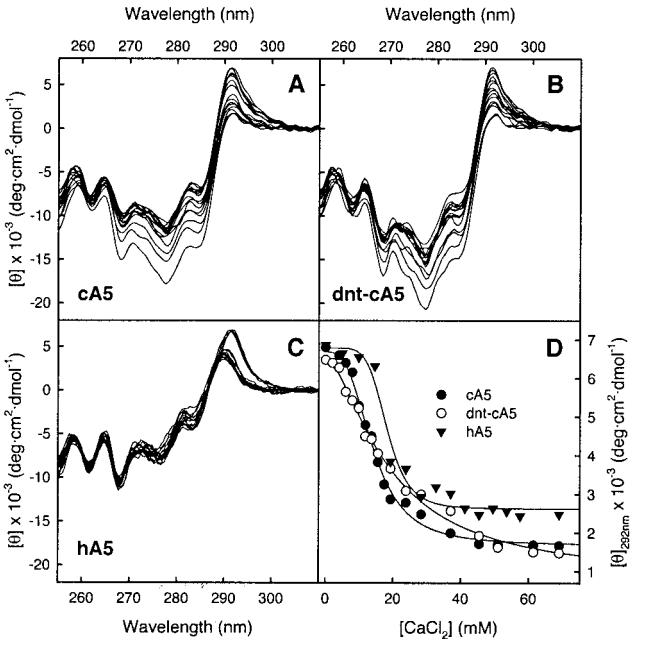

FIGURE 3 Effect of increasing calcium concentration in the near-UV circular dichroism spectra of recombinant annexins. Spectra (*A–C*) were recorded between 250 and 350 nm in a 0.5 cm optical pathlength cuvette and are represented as total ellipticity values. Protein concentration was ~2 mg/ml. Calcium concentration was increased up to 70 mM by addition of the corresponding volumes of a 0.5 M $CaCl_2$ stock solution in the same buffer. After each addition, ellipticity at 292 nm was monitored. Spectra were recorded after equilibrium was reached. All spectra were corrected by subtracting the ellipticity of each buffer. Changes in the total ellipticity at 292 nm in dependence of calcium concentration are also shown (*D*), and were adjusted by nonlinear regression to logistic functions. The different spectra were recorded at the calcium concentrations indicated in *D*.

observed in cA5 and dnt-cA5 in the 265-290 nm region and in the maximum at 292 nm. hA5 also presents significant variations in the maximum at 292 nm, but almost no changes are detected in the minima.

The effect of calcium was monitored by recording the near-UV CD spectra at increasing calcium concentrations after equilibrium was reached; the variations in molar ellipticity at 292 nm are shown also in Fig. 3 *D*. As observed, a continuous decrease in the ellipticity maximum is detected parallel to the increase in calcium concentration. While no change in the position of the maximum at 292 nm is detected in the chicken proteins, a gradual shift toward 290 nm is observed in the human protein. Saturation of the calcium effect on W^{187} ellipticity is achieved at 40–50 mM $CaCl_2$ (~800:1, Ca^{2+}/protein molar ratio) for the wild-type proteins, but higher concentrations are required for the truncated mutant. The half-maximal effect of calcium is achieved at a lower concentration for intact cA5 (14.1 ± 0.4 mM), while it is quite similar for hA5 and the chicken truncated mutant (18.2 ± 0.8 and 18.9 ± 1.5 mM, respectively) as calculated from the nonlinear regression of the

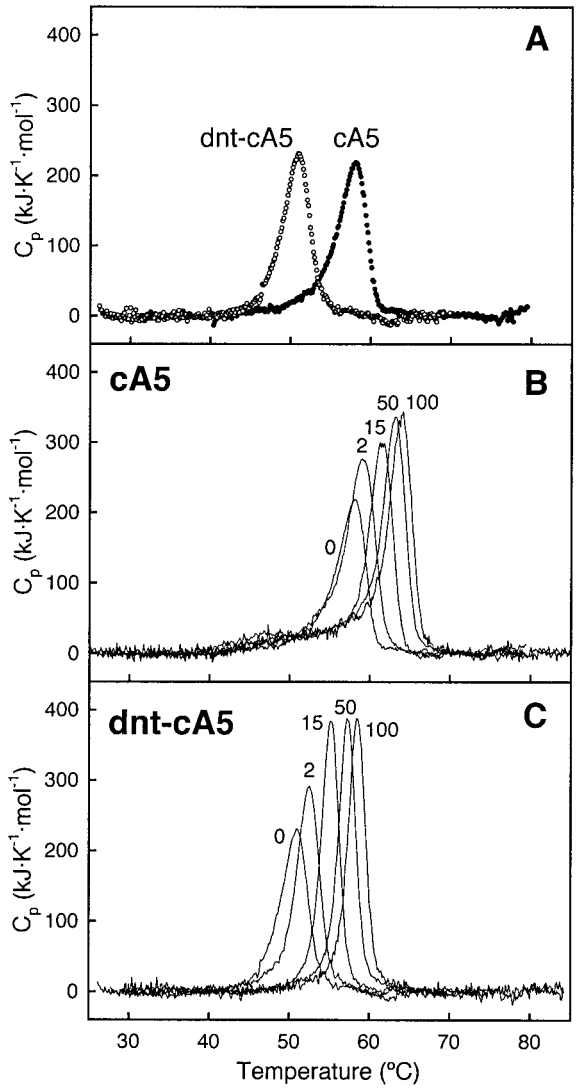

FIGURE 4 Differential scanning calorimetry of cA5 and dnt-cA5. Thermal denaturation of the proteins was analyzed in the absence of calcium (*A*) or in the presence of 2, 15, 50, and 100 mM $CaCl_2$ (*B* and *C*). A second set of scans obtained after thermal unfolding of the proteins were used as baselines due to the irreversibility of the unfolding process.

experimental data to a four-parameter logistic function using SigmaPlot software (SPSS).

Binding of calcium to annexin A5 followed by differential scanning calorimetry

Fig. 4 shows heat capacity scans of cA5 and dnt-cA5 in the absence (Fig. 4 *A*) or at increasing free calcium concentrations ranging from 0 to 100 mM (Fig. 4, *B* and *C*). Numerical integration of these C_p transition curves and the determination of the van't Hoff enthalpy according to Eq. 1 yield the parameters summarized in Table 2. In all cases, the unfolding of the recombinant proteins was followed by an irreversible step, as no transition peaks were obtained in the second heating of the samples at the different calcium concentrations. However, as observed in Fig. 4, the peaks were not highly asymmetric and no exothermic phenomena were observed. Thus, under these experimental conditions, thermodynamic parameters could be calculated (Sánchez-Ruiz et al., 1988; Vogl et al., 1997; Rosengarth et al., 1999) and compared (Table 2). In general, transition peaks were more symmetric for the dnt-cA5 than for the wild-type protein. Increasing concentrations of calcium induce a rise in $t_{1/2}$ from 58.1°C to 64.1°C and from 50.9°C to 58.4°C in the wild-type protein and in the truncated mutant, respectively. These values are in good accordance with those obtained following the disappearance of α-helical secondary structure by CD spectroscopy. The cooperativity ratio $\Delta H_{cal}/\Delta H_{vH}$ (Table 2) was close to 1 in the truncated mutant; however, this parameter was far from 1 in cA5. Thus, thermal transitions could not be adjusted to a simple two-state model, as occurs for the human annexins A5 and A1 (Vogl et al., 1997; Rosengarth et al., 1999).

TABLE 2 Variation of thermodynamic transition parameters of chicken annexin A5 and dnt-cA5

$[CaCl_2]$ (mM)	$t_{1/2}$ (°C)	ΔH_{cal} (kJ·mol^{-1})	ΔH_{vH} (kJ·mol^{-1})	$\Delta H_{cal}/\Delta H_{vH}$
cA5				
0	58.1	1152	693	1.66
2	59.0	1548	654	2.37
15	61.2	1563	714	2.19
50	63.2	1794	705	2.54
100	64.1	1820	716	2.54
dnt-cA5				
0	50.9	1045	773	1.35
2	52.6	1198	859	1.39
15	55.1	1209	1139	1.06
50	57.2	1302	1081	1.20
100	58.4	1313	1080	1.22

Data correspond to a representative experiment of three independent, almost identical, measurements.

Characterization of recombinant annexins by IR spectroscopy

Protein structure can be studied by IR spectroscopy through decomposition of the original amide I band located between 1700 and 1600 cm^{-1}. The deconvolved spectra of the amide I band corresponding to the three samples studied in the absence and the presence of 100 mM calcium are shown in Fig. 5. The spectrum corresponding to cA5 in a D_2O medium shows five peaks centered at around 1680, 1666, 1651, 1634, and 1612 cm^{-1}. The spectra corresponding to the dnt-cA5 and to hA5 also show peaks at similar positions. No big changes are observed on the lineshape of the deconvolved spectra in the three proteins. However, saturation of the three proteins with 100 mM calcium induces alterations in the IR spectra (Fig. 5) with an overall shift of the spectra toward higher wavenumbers. These changes can be sum-

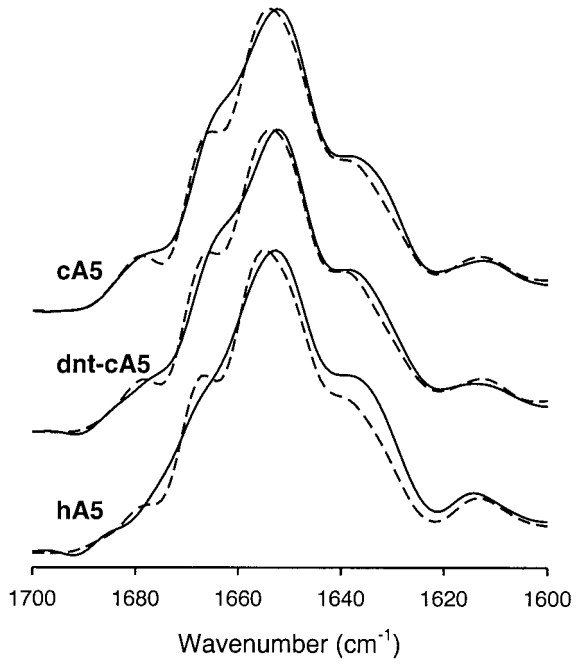

FIGURE 5 Deconvolved IR spectra of the amide I band of recombinant annexins. IR spectra of cA5, dnt-cA5, and hA5 were recorded in the absence (*solid lines*) or presence (*dashed lines*) of 100 mM $CaCl_2$ at 25°C. The deconvolved region between 1600 and 1700 cm^{-1} is shown.

marized in shifts of the maximum band at 1651 to 1655 cm^{-1} and from 1634 to 1637 cm^{-1}, and lineshape changes in the region around 1666 cm^{-1}.

The amount of the different structures can be obtained by decomposition of the amide I band (Byler and Susi, 1986; Arrondo and Goñi, 1999). The values for the band components of the different annexins herein studied, in the absence and presence of calcium, are shown in Table 3. The helical component in wild-type and dnt-cA5 chicken annexins, represented by the bands at 1651 and 1634 cm^{-1}, is very similar, ~69%, and not very different from that obtained from far-UV CD spectroscopy. Human annexin shows a slight increase (~5%) in its α-helical content and a concomitant decrease in the contribution of vibrations at around 1680 cm^{-1}. In the presence of 100 mM calcium, a similar effect is seen in the three proteins: an increase in the α-helical content and a decrease in the turn or 3_{10} helix content (1666 cm^{-1}). The band around 1680 cm^{-1}, which does not change in the different samples studied, can be possibly attributed to the high-frequency component of the interacting chains or to turns.

Thermal denaturation of annexin A5 followed by IR spectroscopy

Protein thermal denaturation is characterized in IR spectroscopy by the appearance of two characteristic bands around 1620 cm^{-1} and 1685 cm^{-1} due to protein aggregation. This allows the characterization of the thermal denaturation profiles by looking at the width of the amide I band (Arrondo and Goñi, 1999). Fig. 6 shows the thermal profiles of the amide I bandwidth corresponding to the different annexins in the absence or presence of 100 mM calcium. The values obtained for the T_m by this procedure in the absence of calcium are also shown in Fig. 6. A significant increase in this parameter after calcium binding is observed, being larger for hA5 (~11°C) than for dnt-cA5 (~7°C) and cA5 (~5°C). These values are similar to those obtained by far-UV CD spectroscopy (Fig. 2).

It is also possible to monitor the temperature-induced changes by looking at the 2D-IR correlation spectra, which can reveal small changes in the spectra, and also the interaction between the two bands that account for these changes. In synchronous spectra, the peaks located in the diagonal (autopeaks) correspond to changes in the intensity, induced in this case by temperature, and are always positive. The cross-relation peaks indicate a relationship between the two bands involved. Fig. 7 shows the synchronous spectra corresponding to annexins in the absence (Fig. 7, *A* and *C*) and in the presence (Fig. 7, *B* and *D*) of 100 mM Ca^{2+} when the temperature range 25–80°C is analyzed by 2D-IR. A prominent peak appears located around 1618 cm^{-1}, which corresponds to the aggregation band; faint peaks are observed at 1655 and 1685 cm^{-1}, indicating also the involvement of these bands in the protein denaturation. When the cross-relation peaks are considered, a negative correlation between the bands at 1655 and at 1618 cm^{-1} indicates that the rise in the aggregation band is due to the decrease in α-helix. Almost identical profiles were obtained for dnt-cA5 when compared to the wild-type protein (not shown). Human annexin also shows a very similar pattern to the chicken counterpart (Fig. 7, *C* and *A*, respectively). However, if calcium is added to the protein preparations, not only a more intense autopeak is detected at 1655 cm^{-1}, but new cross-relation bands are produced, like the negative relation between 1665 and 1618 cm^{-1} and the positive correlation between the band at 1655 cm^{-1} and the one at 1665 cm^{-1}, indicating that in the presence of calcium the denaturation is more complex and involves other structures.

We have also performed the 2D-IR correlation analysis in the interval 25–40°C to check structural rearrangements before denaturation takes place. Autopeaks and correlation peaks are observed in chicken annexin at 1634 and 1655 cm^{-1} (Fig. 8), showing a negative correlation between them. This would indicate that the band at 1634 cm^{-1} relates to α-helices and that helix-helix interactions change before denaturation begins. The pattern is alike for the protein in the presence or the absence of calcium but the intensity of the correlation peaks is different, demonstrating again that in the presence of calcium protein conformation is altered. Mutant dnt-cA5 and human annexin present a similar 2D-IR peak pattern to wild-type cA5 in this temperature range.

TABLE 3 Secondary structure percentage corresponding to the amide I band decomposition of chicken and human annexin A5 IR spectra in the absence and presence of 100 mM $CaCl_2$

	Amide I Frequency Range (cm^{-1})				
	1651–1655	1634–1638	1665–1668	1677–1680	Total α-helix
cA5	40	29	20	11	69
cA5 + 100 mM $CaCl_2$	55	27	8	10	82
dnt-cA5	33	36	23	8	69
dnt-cA5 + 100 mM $CaCl_2$	53	29	8	10	82
hA5	40	34	21	5	74
hA5 + 100 mM $CaCl_2$	60	27	4	9	87

Values are taken from the amide I band decomposition. Band assignments are discussed in the text. The total α-helical percentage was assumed to be the addition of the contributions of vibrations at 1651–1655 cm^{-1} and 1634–1638 cm^{-1}. Data are the average of four different spectra.

DISCUSSION

To understand the functionality of annexins, a better knowledge of the structure-function relationship in these proteins is required. Even though there is a great sequence homology in the core of annexins, small differences may account for significant structural and/or thermodynamic variations that may have an important impact on some of the differential functions exerted by different annexins. Previous studies by Rosengarth et al. (1999) comparing energetics of rat annexin A1 and hA5 revealed that these two proteins, which present a 50% sequence identity, show remarkable differences in stability parameters. Here we show that hA5 and cA5, with 78.1% sequence identity and 86.9% sequence homology, present also a very different thermal stability and behavior, which strongly suggests that the physiological role of annexins may differ not only from one annexin to other, but also among the same members of this protein family in species with enough evolutionary distance.

We have analyzed the role of the N-terminus in the stabilization of the annexin structure by comparing wild-type cA5 with the already described mutant dnt-cA5, which lacks amino acid residues 3-10 (Turnay et al., 1995; Arboledas et al., 1997). No differences in the far-UV CD and IR spectra between the chicken recombinant proteins can be observed; however, the partial truncation of the N-terminus induces a significant decrease ($\sim$7°C) in the melting temperature of the protein by both techniques. Thus, even though the N-terminal extension is essential for specific functions of annexins, it is not required for the correct folding of chicken annexin A5; however, this region strongly contributes to stabilizing the overall structure of annexin A5 by establishing interactions between the first and fourth domains, closing the ring-shaped structure of the molecule.

The effect of calcium binding detected in wild-type cA5 can be also observed in dnt-cA5, inducing a stabilization of the core structure. Anyway, the 7–8°C difference in protein thermal stability remains as deduced from the melting curves followed by monitoring changes in molar ellipticity at 222 nm and IR amide I bandwidth, and in DSC heat capacity profiles. The half-maximal effect of calcium is reached at concentrations in the same range, even though it is slightly lower for the wild-type protein. DSC analyses also show differences that may be considered significant: peaks are more symmetric and the ratio $\Delta H_{cal}/\Delta H_{vH}$ is closer to 1 for the dnt-cA5. Since the simple two-state denaturing model cannot be applied to cA5 or its mutant, it is difficult to obtain more information from these data. However, the differences detected between these two proteins, and with hA5 (Vogl et al., 1997) and rat annexin A1 (Rosengarth et al., 1999), makes it worth further analysis.

In the absence of calcium, cA5 and hA5 differ slightly in their CD and IR spectra. However, significant changes are detected in the melting point, showing human annexin a lower thermal stability than its chicken counterpart (7.6°C and 8.1°C by CD and IR spectroscopy, respectively). Moreover, the shape of the CD melting curve is rather different: hA5 presents a tableau between 55°C and 57°C that does not appear in cA5, and could correspond to an intermediate form in the denaturing process. The main structural feature in the protein at 57°C corresponds to β-sheet, typical of denatured proteins. Thus, it is possible that the further increase in ellipticity at 222 nm up to 75°C may be originated by protein aggregation after unfolding. In fact, the biphasic behavior disappears when ionic strength is increased without modifications in the CD spectrum at 25°C, as also observed for low calcium concentrations (lower than 5 mM); the final denatured state of the protein is also different from that obtained in the presence of calcium. When the melting curve of hA5 is analyzed by IR spectroscopy following amide I bandwidth, the putative intermediate state in the absence of calcium does not appear, and only a highly cooperative transition can be observed. Taking into account that IR spectroscopy is much less dependent on artifacts due to protein aggregation or precipitation, it can be suggested that the tableau that appears in the CD melting curve in the absence of calcium corresponds to the completely unfolded state; further transitions may be nothing more than artifacts due to aggregation or precipitation.

IR spectroscopy has been useful for the determination of the secondary structure of proteins, complementing and providing, in some cases, additional information to CD

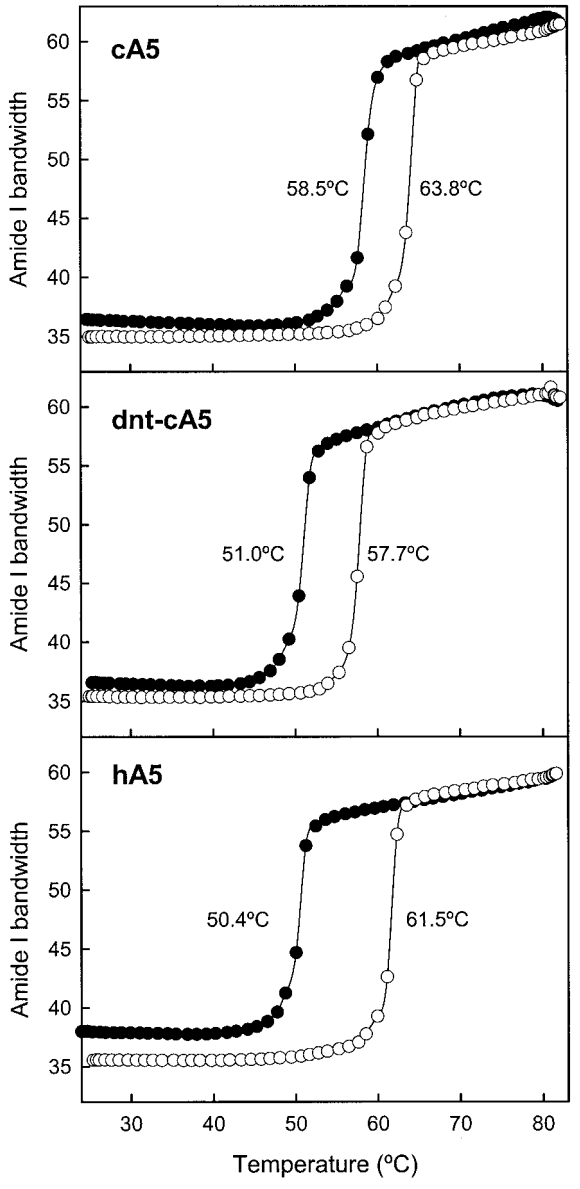

FIGURE 6 Thermal denaturation of recombinant annexins following the amide I bandwidth of the IR spectra. The behavior of the amide I IR band with increasing temperatures was followed by measuring its width at half-height. Thermal amide I bandwidth profiles are shown for cA5, dnt-cA5, and hA5 in the absence (*filled circles*) or in the presence (*open circles*) of 100 mM $CaCl_2$.

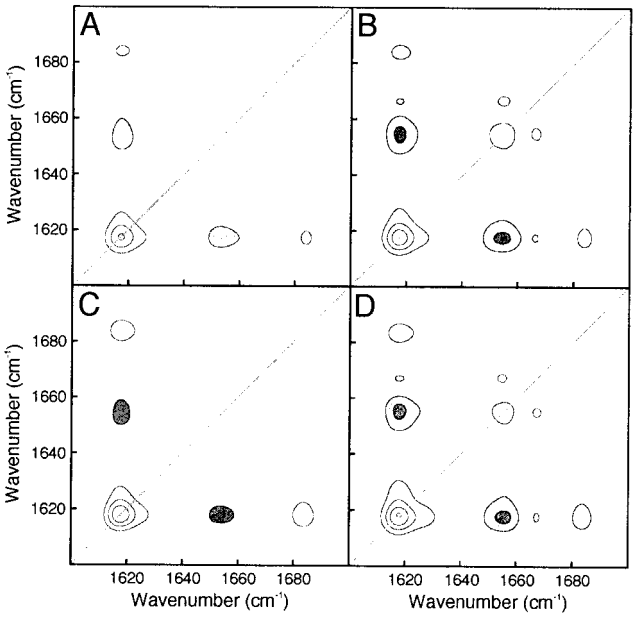

FIGURE 7 Synchronous (Φ) 2D-IR map of annexins. Correlation maps in the absence (*A* and *C*) or presence (*B* and *D*) of 100 mM $CaCl_2$ were recorded for cA5 (*A* and *B*) and hA5 (*C* and *D*) in the temperature interval 25–80°C. Shadowed bands correspond to negative correlation peaks and white to positive correlation peaks. The contour maps do not show small peaks below the established threshold.

spectroscopy. This technique has been already used for the study of conformational changes that take place in human annexin A5 after binding to anionic phospholipid membranes (Silvestro and Axelsen, 1999; Wu et al., 1999). Band assignment is not yet a straightforward procedure because of the sensitivity of IR spectroscopy, and a stepwise method must be followed (Arrondo and Goñi, 1999). First, the assignment of well-defined bands is accomplished and, then, the bands presenting any problems are discussed. From the bands observed in the recombinant proteins, the one at 1612 cm^{-1} arises from amino acid side chains, the one around 1651 cm^{-1} can be attributed to canonical α-helix, and the band at 1666 cm^{-1} in a D_2O medium to turns, or to short or 3_{10} helices (Arrondo and Goñi, 1999). Vibrations at 1634 together with 1680 cm^{-1} in a D_2O medium are normally attributed to β-sheets (Arrondo et al., 1993), but they have also been assigned to short, extended structures connecting α-helices (Byler and Susi, 1986). However, a band around 1635 cm^{-1} was described in an all-alpha protein like myoglobin (Torii and Tasumi, 1992). In addition, it was found that coiled coils generate bands in this region that were assigned to helix-helix interaction (Reisdorf and Krimm, 1996). Gilmanshin et al. (1997) also describe the appearance of two different populations of α-helical structures in apomyoglobin: the canonical α-helices (1650 cm^{-1}) protected from the solvent by tertiary interactions, and the solvated α-helices, at 1633 cm^{-1}. From the normal IR spectra it is not possible to distinguish whether a band at around 1634 cm^{-1} is due to β-sheet or arises from helical structures. However, no β-sheets are observed in the crystal structure of annexin A5 and we have only detected around 40% of canonical α-helical vibrations (~1650 cm^{-1}), whereas CD spectroscopy yields a 70–80% of α-helix content. In addition, the band at 1634 cm^{-1} appears to arise from noncanonical α-helical components because the 2D-IR synchronous correlation spectra reveal a relationship between this band and that of canonical α-helix. A similar behavior has also been described in Ca^{2+}-ATPase, where a

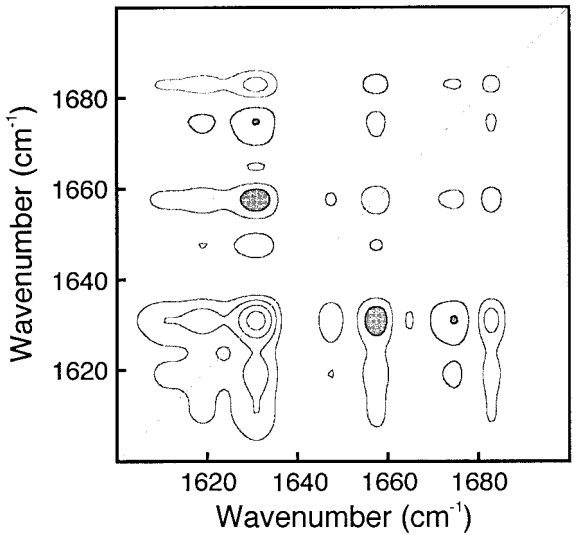

FIGURE 8 Synchronous (Φ) 2D-IR map of chicken annexin A5 before denaturation. The correlation map of cA5 in the absence of calcium in the temperature interval 25–40°C is shown. Shadowed bands correspond to negative correlation peaks and white to positive correlation peaks.

band at a wavenumber lower than that of the canonical α-helix in the thermal denaturation pattern shifts to a normal helix frequency before aggregation (Echabe et al., 1998).

Calcium binding rapidly induces small but significant changes in the shape of the far-UV CD spectra of cA5 and hA5; these changes are consistent with a slight increase in α-helix content. More evident changes are observed by IR spectroscopy, confirming the increase in the canonical α-helix percentage upon calcium binding due to a reorganization of the vibrations represented by the band around 1666 cm^{-1}, which would correspond to short segments or to 3_{10} helices that rearrange after calcium binding. To verify this fact, we have compared the crystal structures of domain III of hA5 without (Fig. 9 *A*) (Huber et al., 1992) or with (Fig. 9 *C*) calcium bound (Sopkova et al., 1993). A significant increase in the length of helix 3D can be observed after calcium binding, changing from a short 3_{10} helical structure (Bewley et al., 1993) to a longer α-helix. If this conformational change takes place in the four domains, it could account for the changes detected in IR and far-UV CD spectra. Even though the crystal structure of domain III of cA5 is not known with calcium bound, it can be suggested that similar changes take place upon calcium binding in view of the similarity of the structure in the absence of calcium (Fig. 9 *B* compared to Fig. 9 *A*). According to the 2D-IR correlation maps, the changes observed in the structure prediction from the IR spectra could also be due to the orientation of the α-helices that suffers reorganization, as shown in the scheme in Fig. 9 *D*. All these structural changes after calcium binding lead to a more compact overall tertiary structure that could account for the increased thermostability of the proteins and the shift toward higher

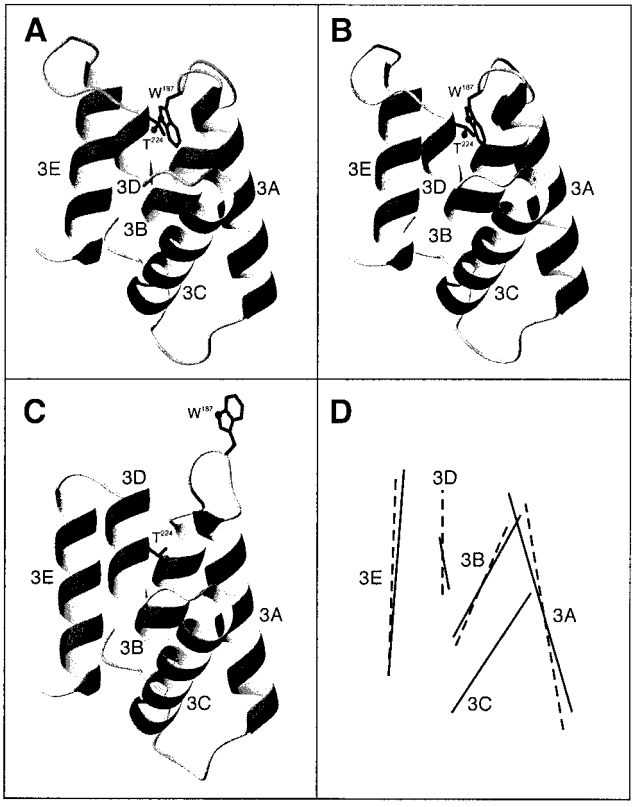

FIGURE 9 Ribbon representation of the three-dimensional structures of the two conformational states of domain III of annexin A5. Domain III of human annexin A5 without calcium (*A*) (Huber et al., 1992) or with calcium bound (*C*) (Sopkova et al., 1993), and chicken annexin A5 without calcium bound (*B*) (Bewley et al., 1993) is shown. Tryptophan 187 (W^{187}) is represented in the calcium-free (*A* and *B*) and calcium-bound (*C*) conformations. A scheme of the rearrangement of the α-helices in domain III of human annexin A5 upon calcium binding is shown in *D*; helix 3C was used for alignment of the structures. Note that the main changes upon calcium binding affect the length of helix 3D and induces changes in the orientation of the helices. The figures were prepared using the MOLMOL program (Koradi et al., 1996).

wavenumbers in the IR spectra due to a more difficult hydrogen-deuterium exchange (Muga et al., 1991).

When the effect of calcium is analyzed by CD in the near-UV region, the main changes in hA5 and cA5 affect to the maximum at 292 nm. This is a direct consequence of the local conformational change that affects the AB loops upon calcium binding in the high-affinity sites exposing residues M^{31} (L^{31} in human), A^{103}, W^{187}, and A^{262} to the solvent or to the interacting biological membranes (Berendes et al., 1993; Concha et al., 1993; Sopkova et al., 1993, 1998; Follenius-Wund et al., 1997; Pigault et al., 1999). The W^{187} residue of domain III is located in a hydrophobic pocket and interacts through hydrogen bonds with T^{224} (Bewley et al., 1993; Sopkova-de Oliveira Santos et al., 2000, 2001) in both human and chicken proteins. This interaction blocks the conformational mobility freedom of this residue and thus, a maximum at 292 nm appears in the near-UV CD

spectrum. After calcium binding, the interaction of W^{187} with T^{224} is broken (Sopkova-de Oliveira Santos et al., 2000, 2001) and W^{187} is exposed to the solvent, as it is clearly observed comparing Fig. 9 *A* and 9 *C* based on the crystal structures of human annexin A5 without or with calcium bound to this domain (Huber et al., 1992; Sopkova et al., 1993). As a direct consequence of the increase in mobility, ellipticity at 292 nm decreases. Thus, changes in this maximum allow the determination of calcium binding to this particular domain. In the absence of phospholipids, the calcium concentrations required for the conformational change to take place are much higher than in their presence (Meers, 1990; Meers and Mealy, 1993; Sopkova et al., 1994; Arboledas et al., 1997). At these Ca^{2+}/protein molar ratios, the apparent K_d for calcium can be considered almost identical to the calcium concentration required to obtain the half-maximal effect on W^{187} (10–20 mM). Thus, affinity for calcium in the absence of phospholipids is approximately three orders of magnitude lower than in the presence of phospholipids (Raynal and Pollard, 1994). The calcium-dependent change in ellipticity at 292 nm due to W^{187} is highly cooperative in the wild-type proteins, showing cA5 a slightly lower calcium requirement than its human counterpart (half maximal effect at 14.1 ± 0.4 vs. 18.2 ± 0.8 mM $CaCl_2$, respectively). Even though the N-terminal extension of annexins is located on the opposite site of the annexin molecule, its truncation affects the calcium binding site in domain III. On this idea, the calcium-dependent change in ellipticity at 292 nm in dnt-cA5 is not as cooperative as that in the chicken wild-type protein. These results are in good accordance with those previously reported by our group showing that the truncated mutant presents a more relaxed conformation with an increased exposure of W^{187}, and that both cA5 and dnt-cA5 expose W^{187} after calcium binding based on a red-shift with a parallel increase in quantum yield of their fluorescence emission spectra (Arboledas et al., 1997). All these results support the hypothesis that the conformational changes that take place on domain III of hA5 also occur in the chicken protein, being responsible for the observed changes upon calcium binding detected by far-UV CD and IR spectroscopy.

From the results herein presented it could be concluded that avian and human annexins significantly differ in their thermal stability even though there is a high degree of sequence identity and homology between them. In fact, the stability of hA5 is equivalent to that of the dnt-cA5, where almost all the N-terminal extension is missing. However, in the protein from both species, calcium induces similar effects and the differences between chicken and human become less significant. We have detected interesting conformational changes after saturation of the proteins with calcium in solution by CD spectroscopy, but these changes are much more obvious when analysis of the amide I band is performed by curve-fitting and 2D-IR. This technique appears to be able to detect unequivocally the conformational rearrangements that take place after calcium saturation, which were previously reported based on the crystal structures of hA5 (Huber et al., 1992; Sopkova et al., 1993). Calcium binding induces secondary structure changes that affect the length of helices D and induces rearrangements among the helix bundles affecting helix-helix interactions with concomitant changes in the tertiary structure of the protein.

We are grateful to Dr. M. P. Fernández (University of Oviedo, Spain), for kindly providing a cDNA clone for human annexin A5, and to Dr J. Villalaín (University Miguel Hernandez, Spain) and Dr. M. Pezolet (University Laval, Canada), for providing us the 2D algorithm.

This work was supported by Grants PM98-0083 from the DGES (Spain), G03/98 from the University of Basque Country, and PI 1998-33 from the Basque Government.

REFERENCES

Arboledas, D., N. Olmo, M. A. Lizarbe, and J. Turnay. 1997. Role of the N-terminus in the structure and stability of chicken annexin V. *FEBS Lett.* 416:217–220.

Arrondo, J. L. R., and F. M. Goñi. 1999. Structure and dynamics of membrane proteins as studied by infrared spectroscopy. *Prog. Biophys. Mol. Biol.* 72:367–405.

Arrondo, J. L. R., A. Muga, J. Castresana, and F. M. Goñi. 1993. Quantitative studies of the structure of proteins in solution by Fourier-transform infrared spectroscopy. *Prog. Biophys. Mol. Biol.* 59:23–56.

Berendes, R., A. Burger, D. Voges, P. Demange, and R. Huber. 1993. Calcium influx through annexin V ion channels into large unilamellar vesicles measured with fura-2. *FEBS Lett.* 317:131–134.

Bewley, M. C., C. M. Boustead, J. H. Walker, and R. Huber. 1993. Structure of chicken annexin V at 2.25A resolution. *Biochemistry.* 32: 3923–3928.

Böhm, B. B., B. Wilbrink, K. E. Kuettner, and J. Mollenhauer. 1994. Structural and functional comparison of anchorin CII (Cartilage Annexin V) and muscle annexin V. *Arch. Biochem. Biophys.* 314:64–74.

Byler, D. M., and H. Susi. 1986. Examination of the secondary structure of proteins by deconvolved FTIR spectra. *Biopolymers.* 25:469–487.

Concha, N. O., J. F. Head, M. A. Kaetzel, J. R. Dedman, and B. A. Seaton. 1993. Rat annexin V crystal structure: Ca(2+)-induced conformational changes. *Science.* 261:1321–1324.

Contreras, L. M., F. J. Aranda, F. Gavilanes, J. M. González-Ros, and J. Villalain. 2001. Structure and interaction with membrane model systems of a peptide derived from the major epitope region of HIV protein gp41: implications on viral fusion mechanism. *Biochemistry.* 40:3196–3207.

Echabe, I., U. Domberger, A. Prado, F. M. Goñi, and J. L. R. Arrondo. 1998. Topology of sarcoplasmic reticulum Ca^{2+}-ATPase: an infrared study of thermal denaturation and limited proteolysis. *Protein Sci.* 7:1172–1179.

Follenius-Wund, A., E. Piemont, J. M. Freyssinet, D. Gerard, and C. Pigault. 1997. Conformational adaptation of annexin V upon binding to liposomes: a time-resolved fluorescence study. *Biochem. Biophys. Res. Commun.* 234:111–116.

Gerke, V., and S. E. Moss. 2002. Annexins: from structure to function. *Physiol. Rev.* 82:331–371.

Gilmanshin, R., S. Williams, R. H. Callender, W. H. Woodruff, and R. B. Dyer. 1997. Fast events in protein folding: relaxation dynamics and structure of the I form of apomyoglobin. *Biochemistry.* 36: 15006–15012.

Hofmann, A., J. Benz, S. Liemann, and R. Huber. 1997. Voltage dependent binding of annexin V, annexin VI and annexin VII-core to acidic phospholipid membranes. *Biochim. Biophys. Acta.* 1330:254–264.

Huber, R., R. Berendes, A. Burger, M. Schneider, A. Karshikov, H. Luecke, J. Römisch, and E. Pâques. 1992. Crystal and molecular structure of human annexin V after refinement. Implications for structure, membrane binding and ion channel formation of the annexin family of proteins. *J. Mol. Biol.* 223:683–704.

Huber, R., M. Schenider, I. Mayr, J. Römisch, and E. P. Pâques. 1990. The calcium binding sites in human annexin V by crystal structure analysis at 2.0 Å resolution. *FEBS Lett.* 275:15–21.

Koradi, R., M. Billeter, and K. Wüthrich. 1996. MOLMOL: a program for display and analysis of macromolecular structures. *J. Mol. Graph.* 14: 51–55.

Laemmli, U. K. 1970. Cleavage of structural proteins during the assembly of the head of bacteriophage T4. *Nature.* 227:680–685.

Liemann, S., J. Benz, A. Burger, D. Voges, A. Hofmann, R. Huber, and P. Göttig. 1996. Structural and functional characterisation of the voltage sensor in the ion channel human annexin V. *J. Mol. Biol.* 258:555–561.

Liemann, S., and R. Huber. 1997. Three-dimensional structure of annexins. *Cell. Mol. Life Sci.* 53:516–521.

López Mayorga, O., and E. Freire. 1987. Dynamic analysis of differential scanning calorimetry data. *Biophys. Chem.* 27:87–96.

Matsuda, R., N. Kaneko, and Y. Horikawa. 1997. Presence and comparison of Ca^{2+} transport activity of annexins I, II, V, and VI in large unilamellar vesicles. *Biochem. Biophys. Res. Commun.* 237:499–503.

Meers, P. 1990. Location of tryptophans in membrane-bound annexins. *Biochemistry.* 29:3325–3330.

Meers, P., and T. Mealy. 1993. Calcium-dependent annexin V binding to phospholipids: stoichiometry, specificity, and the role of negative charge. *Biochemistry.* 32:11711–11721.

Muga, A., H. H. Mantsch, and W. K. Surewicz. 1991. Membrane binding induces destabilization of cytochrome c structure. *Biochemistry.* 30: 7219–7224.

Paquet, M. J., M. Laviolette, M. Pezolet, and M. Auger. 2001. Two-dimensional infrared correlation spectroscopy study of the aggregation of cytochrome c in the presence of dimyristoylphosphatidylglycerol. *Biophys. J.* 81:305–312.

Perczel, A., K. Park, and G. D. Fasman. 1992. Analysis of the circular dichroism spectrum of proteins using the convex constraint algorithm: a practical guide. *Anal. Biochem.* 203:83–93.

Pigault, C., A. Follenius-Wund, and M. Chabbert. 1999. Role of Trp-187 in the annexin V-membrane interaction: a molecular mechanics analysis. *Biochem. Biophys. Res. Commun.* 254:484–489.

Rand, J. H. 1999. "Annexinopathies": a new class of diseases. *N. Engl. J. Med.* 340:1035–1036.

Raynal, P., and H. B. Pollard. 1994. Annexins: the problem of assessing the biological role for a gene family of multifunctional calcium- and phospholipid-binding proteins. *Biochim. Biophys. Acta.* 1197:63–93.

Reisdorf, W. C., and S. Krimm. 1996. Infrared amide I′ band of the coiled coil. *Biochemistry.* 35:1383–1386.

Rosengarth, A., J. Rösgen, H. J. Hinz, and V. Gerke. 1999. A comparison of the energetics of annexin I and annexin V. *J. Mol. Biol.* 288: 1013–1025.

Sable, C. L., and D. W. H. Riches. 1999. Cloning and functional activity of a novel truncated form of annexin IV in mouse macrophages. *Biochem. Biophys. Res. Commun.* 258:162–167.

Sánchez-Ruiz, J. M., J. L. López-Lacomba, M. Cortijo, and P. L. Mateo. 1988. Differential scanning calorimetry of the irreversible thermal denaturation of thermolysin. *Biochemistry.* 27:1648–1652.

Silvestro, L., and P. H. Axelsen. 1999. Fourier transform infrared linked analysis of conformational changes in annexin V upon membrane binding. *Biochemistry.* 38:113–121.

Sopkova, J., J. Gallay, M. Vincent, P. Pancoska, and A. Lewit-Bentley. 1994. The dynamic behavior of annexin V as a function of calcium ion binding: a circular dichroism, UV absorption, and steady-state and time-resolved fluorescence study. *Biochemistry.* 33:4490–4499.

Sopkova, J., M. Renouard, and A. Lewit-Bentley. 1993. The crystal structure of a new high-calcium form of annexin V. *J. Mol. Biol.* 234: 816–825.

Sopkova, J., M. Vincent, M. Takahashi, A. Lewit-Bentley, and J. Gallay. 1998. Conformational flexibility of domain III of annexin V studied by fluorescence of tryptophan 187 and circular dichroism: the effect of pH. *Biochemistry.* 37:11962–11970.

Sopkova-de Oliveira Santos, J., S. Fischer, C. Guilbert, A. Lewit-Bentley, and J. C. Smith. 2000. Pathway for large-scale conformational change in annexin V. *Biochemistry.* 39:14065–14074.

Sopkova-de Oliveira Santos, J., M. Vincent, S. Tabaries, A. Chevalier, D. Kerboeuf, F. Russo-Marie, A. Lewit-Bentley, and J. Gallay. 2001. Annexin A5 D226K structure and dynamics: identification of a molecular switch for the large-scale conformational change of domain 111. *FEBS Lett.* 493:122–128.

Swairjo, M. A., and B. A. Seaton. 1994. Annexin structure and membrane interactions: a molecular perspective. *Annu. Rev. Biophys. Biomol. Struct.* 23:193–213.

Torii, H., and M. Tasumi. 1992. Model calculations on the amide-I infrared bands of globular proteins. *J. Chem. Phys.* 96:3379–3387.

Turnay, J., E. Pfannmüller, M. A. Lizarbe, W. M. Bertling, and K. von der Mark. 1995. Collagen binding activity of recombinant and N-terminally modified annexin V (anchorin CII). *J. Cell. Biochem.* 58:208–220.

Vogl, T., C. Jatzke, H. J. Hinz, J. Benz, and R. Huber. 1997. Thermodynamic stability of annexin V E17G: equilibrium parameters from an irreversible unfolding reaction. *Biochemistry.* 36:1657–1668.

Wu, F., C. R. Flach, B. A. Seaton, T. R. Mealy, and R. Mendelsohn. 1999. Stability of annexin V in ternary complexes with Ca^{2+} and anionic phospholipids: IR studies on monolayer and bulk phases. *Biochemistry.* 38:792–799.